NASA/CR- 97 —   206774

IN-74 CR
055 1 5

LABORATORY MEASUREMENTS OF CELESTIAL SOLIDS

(Final Report)

22 617.

A. J. Sievers

Lab. of Atomic and Solid State Physics and the Center for Radiophysics and Space Research
Cornell University Ithaca, N.Y. 14853

and

S. V. W. Beckwith

Max-Planck-Institut für Astronomie, Königstuhl 17, 69117 Heidelberg, Germany

Period covered: November 1, 1994 to April 30, 1997

I. SUMMARY

Our experimental study has focused on laboratory measurements of the low temperature optical properties of a variety of astronomically significant materials in the infrared and mm-wave region of the spectrum. Our far infrared measurements of silicate grains with an open structure have produced a variety of unusual results: (1) the low temperature mass opacity coefficient of small amorphous $2MgO \cdot SiO_2$ and $MgO \cdot 2SiO_2$ grains are many times larger than the values previously used for interstellar grain material; (2) all of the amorphous silicate grains studied possess the characteristic temperature dependent signature associated with two level systems in bulk glass; and (3) a smaller but nonzero two level temperature dependence signature is also observed for crystalline particles, its physical origin is unclear. These laboratory measurements yield surprisingly large and variable values for the mm-wave absorption coefficients of small silicate particles similar to interstellar grains, and suggest that the bulk absorptivity of interstellar dust at these long wavelengths will not be well known without such studies. Furthermore, our studies have been useful to better understand the physics of the two level absorption process in amorphous and crystalline grains to gain confidence in the wide applicability of these results.

1

II. PROJECT REPORT

A. Management approach

In addition to authoring joint research papers, S. V. W. Beckwith and A. J. Sievers continue to maintain weekly e-mail contact with regard to this experimental program.

B. Personnel

The following additional people have been involved with the research program: one undergraduate - S. Smith; two graduate students - R. Lai and S. A. Jones, and one postdoc - N. Agladze. Some of the silicate samples have been prepared by Professor J. M. Burlitch in the Chemistry Department.

C. Unusual features of the mm-wave properties of silicate grains

1. Background

Knowledge of the optical constants of a number of grain materials is essential to interpret observations of emission and absorption by dust particles, see Refs. [1-7] and references therein). The best estimates of the far IR absorptivity of interstellar grain material [1, 8, 9] generally predict values for the mass opacity coefficient of interstellar particles in the range

$$\kappa_V \approx 0.3 \left(\frac{\tilde{v}}{10cm^{-1}} \right)^{\beta} cm^2g^{-1}, \tag{1}$$

where $\tilde{v} = 1/\lambda$ is the frequency in cm^{-1}, and $\beta = 2$. This value of the index β has been argued on fairly general grounds to apply to the low frequency region of both crystalline [8] and amorphous 3-D materials. On the other hand, for amorphous carbon and layered-lattice silicates, where the phonon density of states is 2-D then the same arguments can be used to predict that $\beta \sim$ 1 [10]. Emerson [8] has shown, using Kramers-Kronig arguments, that $\beta > 1$ in order to be physically acceptable. At the same time, observations of submillimeter wave emission from stars in Taurus and Ophiuchus demonstrate that $\beta \leq 1$ is clearly preferred to fit the spectral distributions [11-14]. Values of $\beta < 2$ are also identified with disks and for large scale distributions of dust in the Galactic plane [15]. Radiative transfer calculations by [16] indicates a similar slow frequency dependence required to understand emission from dense clouds as well. At the same time there are observations in the 100 to 300 μm region indicating a more rapid increase in opacity with frequency, $\beta \sim 2$ (Ref. [17], indicating perhaps that the opacities do not obey a single power law over the entire long wavelength region. In addition, there may be some variation among the different environments (diffuse ISM, cold molecular cloud cores, and circumstellar disks).

Optical constants have been measured in the laboratory for several materials relevant to astronomy over limited wavelength ranges, mainly from optical to infrared wavelengths[18, 19].

2

There are virtually no measurements of the optical properties of the relevant materials at far infrared and mm-wavelengths, especially at temperatures appropriate to the interstellar environment[9]. Since interstellar grains are most likely disordered, an important question is whether or not disorder-related far-infrared bulk processes play a significant role in the far infrared thermal emission from these sources. Such temperature dependent effects are not usually considered when extrapolating short wavelength optical constants to longer wavelengths[3, 8, 17]. Part of our experimental program is to determine whether similar effects occur in small particles of astronomically important materials.

2. Spectral results at low temperatures

Our first broad experimental examination of the low temperature properties of the mm-wave properties of grains has focused on crystalline enstatite and forsterite grains and amorphous silicate grains synthesized by sol-gel reaction (size ~ 0.1 - 1 μm). Their absorptive properties have been measured between 0.7 and 2.9 mm wavelength (3.5 - 15 cm^{-1}) at temperatures between 1.2 and 30 K. The precursor silicate powders were synthesized by a H_2O_2-assisted, sol-gel reaction [20]. Some of the amorphous powders are precursors to forsterite (Mg_2SiO_4) and enstatite ($MgSiO_3$). All of these grains display an open structure. Typically we find that micron scale flakes are made up of fibers of about 25 nm width by 100 nm length. This morphology is consistent with the linear structure indicated by ^{29}Si NMR spectroscopy [21]. Note that because of this open structure, the effective volume fill fraction of the amorphous powder is small. It should be noted that previous far infrared measurements on open structured systems has shown that they tend to adsorb gases from the atmosphere; hence, in order to obtain intrinsic information, the samples must be heated and evacuated before being examined [22]. In the measurements we have made, all the grain samples were evacuated for 1 hour at 150 C before the optical cell was sealed.

The results have provided a number of surprises some of which will be taken up in future work (see Section B). One was that for the amorphous grain substances $MgO \cdot SiO_2$, $2MgO \cdot SiO_2$, and $MgO \cdot 2SiO_2$ at 20 K, the millimeter-wave mass opacity coefficients are found to be up to factors of 0.9, 3.5 and 11 times the [1] values usually adopted for interstellar silicate grains. The measured values at lower temperatures are even larger. In addition, the coefficients are found to depend on the powder production technique.

A summary of some of these results are presented in Figure 1. Figure 1 (a) compares the mass normalized absorption coefficient k = a/r between 3.5 and 15 cm^{-1} (l between 2.9 and 0.7 mm) for forsterite and enstatite powders in the amorphous precursor and crystalline states, for $MgO \cdot 2SiO_2$ in the amorphous state and for bulk soda-lime-silica glass, all at 1.2 K. The largest κ over this frequency region is produced by the amorphous $MgO \cdot 2SiO_2$ powder. The second largest is the $2MgO \cdot SiO_2$ powder.

Figure 1 (b) shows the same data but now corrected so that the single grain mass opacity coefficients k_n are displayed. To do this correction it was necessary for us to extrapolate from the measured composite media sample to the desired single grain configuration. We have derived an analytic expression can be used to connect the two quantities[23].
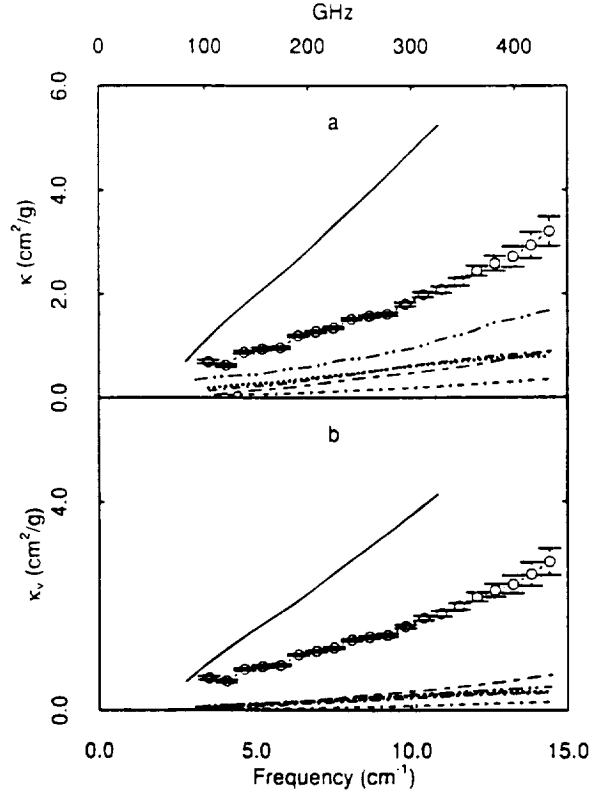
Figure 1. Measured absorption coefficient per unit mass as a function of frequency for amorphous precursor and crystalline forsterite and enstatite powders, amorphous $MgO \cdot 2SiO_2$ and for bulk glass, all at 1.2 K. (a) the mass normalized absorption coefficient, κ. (b) the grain opacity, κ_n, as determined by Eq. 5. Solid line- amorphous $MgO \cdot 2SiO_2$; open circles with error bars - amorphous $2MgO \cdot SiO_2$ powder; dashed-double dotted line – bulk soda-lime-silica glass; dotted line - heat treated (1 hour at 150°C) crystalline powder; dash-dot curve – crystalline forsterite powder without heat treatment. Short-long dashed line - amorphous $MgO \cdot SiO_2$ powder; double dashed-dotted line - heat treated (1 hour at 150°C) crystalline enstatite powder. All powdered samples were evacuated before sealing the optical cell.

The mass opacity coefficient of a grain κ_n can be written in terms of fundamental properties of the material by noting that for spherical particles[8, 17]

$$\kappa_v = \frac{3}{4} \frac{1}{\rho} \frac{Q_{abs}}{a},$$
(2)

where

$$Q_{abs} = 4 \frac{2\pi a}{\lambda} Im\left(\frac{\varepsilon - 1}{\varepsilon + 2}\right) = 4 \frac{2\pi a}{\lambda} Im\left(\frac{-3}{\varepsilon + 2}\right),$$
(3)

4

and $\varepsilon = \varepsilon_1 + i\varepsilon_2$ is the bulk dielectric function of the grain material. For dielectrics, in the limit of low frequencies, ε_1 takes on a large constant value ε_0 while ε_2 becomes small. Hence the approximate expression for the grain absorption efficiency over the grain radius simplifies to

$$\frac{Q_{abs}}{a} = 12\frac{2\pi}{\lambda}\frac{\varepsilon_2}{\left(\varepsilon_1+2\right)^2} = 12\frac{\omega}{c}\frac{\varepsilon_2}{\left(\varepsilon_1+2\right)^2}.$$ (4)

The relation between the mass opacity coefficient of the isolated grain and the mass normalized absorption coefficient $\kappa = \alpha/\rho$ of the measured composite medium in the low frequency limit is obtained from an expansion of a composite media expression for small f. The final result is[23]

$$\frac{\kappa(\omega,f)}{\kappa_v(\omega)} = 1 + \frac{1}{2}\frac{(\varepsilon_0-1)(13\varepsilon_0-10)}{\left(\varepsilon_0+2\right)^2}f + \frac{3}{8}\frac{(\varepsilon_0-1)^2(85\varepsilon_0^2-268\varepsilon_0+81)}{\left(\varepsilon_0+2\right)^4}f^2,$$ (5)

which can be written as

$$\kappa_v(\omega) = g(\varepsilon_0,f)\,\kappa(\omega,f),$$ (6)

where $g(\varepsilon_0, f)$ is the finite concentration reduction factor.

The effective volume fill fraction of the amorphous $MgO\cdot 2SiO_2$ and $2MgO\cdot SiO_2$ powders is small enough that the coefficients in Figure 1(a) can be compared directly with those determined for isolated spherical grains in (b). Samples with larger fill fractions show significant change between the two panels: Soda-lime-silica glass, which is the third strongest absorber in (a), is the fourth from the bottom in (b). The measured k is significantly larger for evacuated powder which had been baked at the same time compared with powder that was sealed at room temperature. The change in the magnitude of κ with heat treatment for crystalline forsterite grains is surprising. This extra contribution may be associated with the grain surfaces, how much of the surface appears amorphous and whether or not they are coated by adsorbed gases. It is noteworthy that *removing the adsorbed gas increases κ.*

The mass opacity coefficients are unexpectedly large for some of these particles. It is noteworthy that at 20 K the absolute value of k_n for amorphous $MgO\cdot 2SiO_2$ is about 11 times larger and amorphous $2MgO\cdot SiO_2$ is about 3.5 times larger than the value normally adopted by astronomers - 0.3 cm^2 g^{-1} - for silicates in interstellar dust. The relatively large coefficients indicate other absorption mechanisms operate at these frequencies in addition to the asymptotic tails of higher frequency resonant processes such as the $\sim$ 10 μm lattice resonances [8].

3. Temperature dependent properties indicative of two level behavior

The temperature dependence of the absorption coefficient per unit mass is somewhat different than that found in bulk crystals in that the absorption at first decreases with increasing temperature until about 20 K and then increases at higher temperatures. This unusual temperature
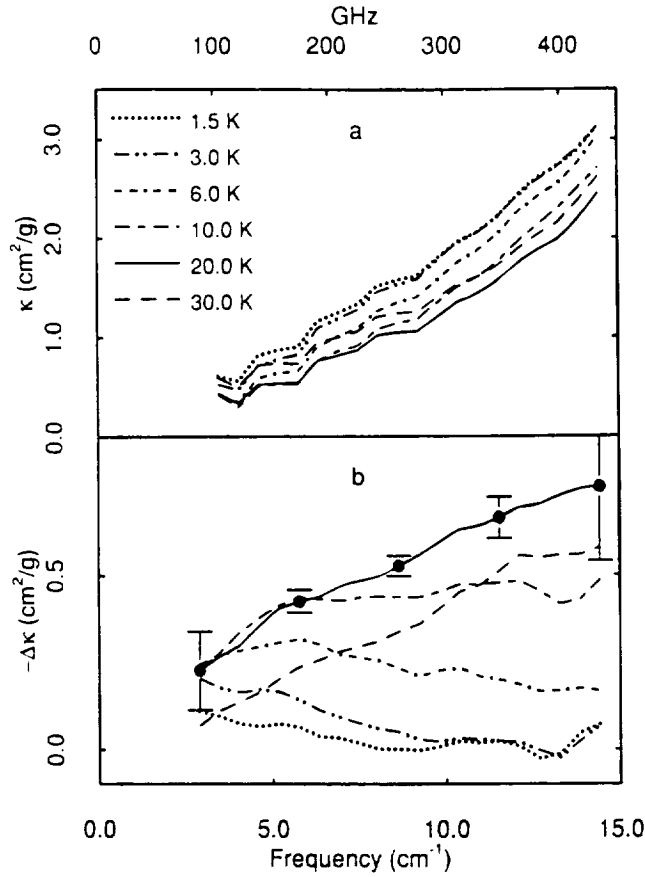
Figure 2. Temperature dependence of the absorption coefficient per unit mass for amorphous 2MgO·SiO$_2$ grains versus frequency. (a) κ as a function of temperature. Over this frequency range κ(T) decreases with increasing temperature up to about 20 K and then increases again at higher temperatures. (b) Difference in κ for specific temperature jumps. The ordinate: —Δκ = [κ(T) — κ(T$_r$)] where T$_r$ = 1.2 K. Typical error bars are given.

dependent property forms a significant part of the overall absorption at long wavelengths and the relative change is as large as 50% at 1 mm wavelength for 2MgO·SiO$_2$, 35% for MgO·SiO$_2$ and 14% for MgO·2SiO$_2$. This temperature dependence of κ is an important diagnostic of the physics governing the absorption process. The frequency dependence of the mass normalized absorption coefficient as a function of temperature is presented in Fig. 2(a). This dependence is most accurately studied as the difference between two spectra acquired at different temperatures. Figure 2(b) shows the temperature dependent results for amorphous 2MgO·SiO$_2$ grains from 1.5 K to 30 K presented as -Δκ = κ(1.2 K) - κ(T) versus frequency. Note that if κ(T) is smaller than κ(1.2 K) at each temperature, then -Δκ is greater than zero as are most of the traces in this figure. This low frequency bleaching behavior of κ(T) with increasing temperature is observed up to about 20 K. At the highest temperature of T = 30 K (dashed curve), the trend is reversed, and the temperature dependent absorption coefficient is now larger than it is at 20 K although still smaller than at 1.2 K. Note that the magnitude of Δκ is larger than the magnitude usually adopted for κ itself for interstellar grains; the temperature dependence is clearly an important characteristic of these amorphous grain materials.

A systematic study of this temperature dependence demonstrates that the results are somewhat similar to those found earlier in bulk glasses. At millimeter wavelengths, amorphous solids show strongly temperature dependent absorption coefficients. At the lowest temperatures, the mm wave absorption coefficient is dominated by a constant spectral density of low lying two level tunneling states [24]. As the temperature increases above 0 K, the absorption *decreases* due to increased population in the excited states [25]. When the temperature gets high enough (a few tens of Kelvin), most of the two level states (TLS) are equally populated and this absorption process becomes extremely weak; however, absorption to the higher excited states of TLS becomes stronger [26]. At still higher temperatures relaxation processes appear to control the absorption coefficient and this effect grows in strength with increasing temperature [27, 28]. The original explanation for these TLS [29] is that atoms and groups of atoms tunnel in the disordered system, but the underlying dynamics behind such states is still not understood and this issue constitutes one of the outstanding problems in condensed matter physics. To illustrate the exact temperature dependence of the absorption coefficient, we write the mass normalized two level absorption coefficient at frequency ω (r/s) and temperature T as[30]:

$$\kappa_{TLS}(\omega) = \frac{4\pi^2 N\mu^2\omega}{c\sqrt{\varepsilon_0}\ \rho_b} \tanh\left(\frac{\hbar\omega}{2kT}\right),\tag{7}$$

where N is the density of states,

$$\mu^2 = \mu_b^2\left(\frac{\varepsilon_0 + 2}{3}\right)^2,\tag{8}$$

is the modulus squared of the effective electric dipole matrix element of the transition between the two states, ε_0 is the dielectric constant, ρ_b the bulk density, c the speed of light and k is Boltzmann's constant. Specific heat measurements on bulk glasses at low temperatures show that N is essentially frequency independent at low frequencies [24]. Fits to the temperature dependent data can be used to determine the temperature independent coefficient in Eq. (7). Our findings for the frequency dependence of the density of states times the dipole moment squared, $N\mu_b^2$, are presented in Figure 3. The value of ε_0 for different olivines varies from 8.4 to 9.5, and we used $\varepsilon_0 = 9$ in the calculations described above. There is no value of ε_0 available for enstatite or for $MgO \cdot 2SiO_2$. so we make use of the dc dielectric constant data for augite, $Ca(Mg,Fe,Al)(Al,Si)_2O_6$, which varies between the limits 6.90-10.27. The value 9, the same as for forsterite, was used for each calculation of the local field correction in Eq. 5. In all the systems studied, Fig. 3 indicates that the ordinate value, $N\mu_b^2$, is nearly independent of frequency. The uncertainties evaluated as mean square deviations from Eq. (7) are smaller than the symbols. As anticipated the measured densities of the crystalline and the amorphous powders are quite different. This significant difference in densities between the particles and the bulk occurs because the amorphous grains have an open aerogel [31] or fractal-like structure. Note the surprising result in Figure 3 that even the crystalline grains show a small degree of two level behavior in the mm-wave region.
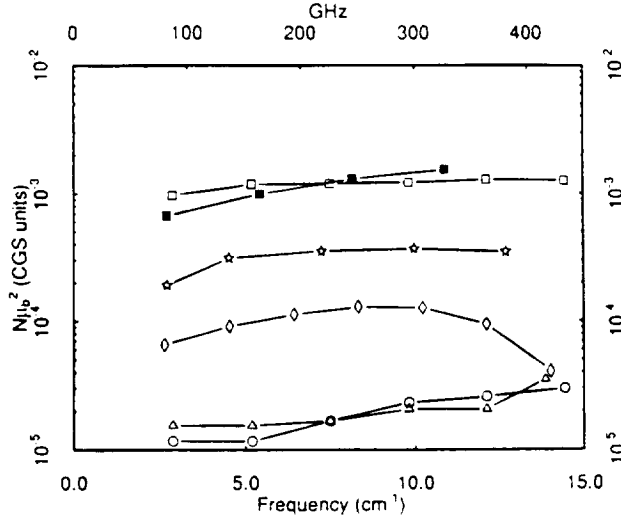
Figure 3. Frequency dependence of the product of the two level density of states times the dipole moment squared versus frequency. Open squares - amorphous $2MgO \cdot SiO_2$ grains; solid squares - amorphous $MgO \cdot 2SiO_2$; stars - amorphous $MgO \cdot SiO_2$ grains; diamonds – bulk soda-lime-silica glass; triangles - heat treated (1 hour at 150°C) crystalline forsterite grains; circles – crystalline forsterite grains without heat treatment.

4. Temperature dependence of the mm-wave index value

Figure 1 shows that κ_n(1.2 K) for amorphous $2MgO \cdot SiO_2$ grains is about six times larger than for the crystalline grains and more than seven times larger than for bulk soda-lime-silica glass, while the value for amorphous $MgO \cdot 2SiO_2$ is quite a bit larger still. This extra dipole strength in the amorphous silicate grain could come from local inhomogeneities. The frequency dependence of the absorptivity of small amorphous grains produced by a charge fluctuation mechanism has been examined by [32], who proposed that the emission efficiency in the long wavelength region would vary as λ^{-1} because of the importance of surface phonon modes. Since a vibrational spectrum is involved in the mechanism[33] , this contribution should be nearly temperature independent, and is in marked contrast with the strongly temperature dependent nature of our experimental data for the mm -wave region. Note that the distribution of two level systems required to explain our results are still outside the framework of lattice dynamics theory. The low temperature data for the amorphous powders can be fitted approximately with a power law as is customary in astronomy, $\kappa_v(\tilde{v}) \sim \tilde{v}^\beta$, with the power law index β as given by Eq. 1; however, because of the temperature dependence of the 2-level density of states, we find that the power law index is temperature dependent. Figure 4 displays the temperature dependence of the power law index over the temperature range investigated as determined by a least squares fit to the data. The values of $\beta(T)$, determined for the amorphous precursor grains of forsterite and enstatite between
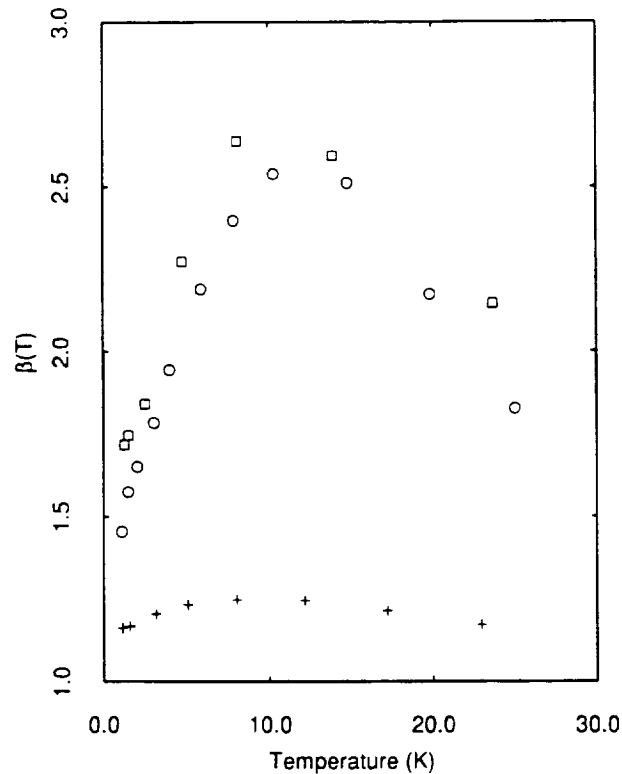
8

Figure 4. Temperature dependence of the power law index $\beta(T)$. Least square fits to the spectra at different temperatures in accord with Eq. (7) in the text are used to determine the $\beta(T)$ values given in the figure. The circles identify the power law fits to the amorphous $2MgO \cdot SiO_2$ spectra, the squares, to the amorphous $MgO \cdot SiO_2$ spectra and the crosses, to the amorphous $MgO \cdot 2SiO_2$ spectra.

5 and 15 cm⁻¹, are remarkably similar: at low temperature the power law index is about 1.5, it then increases to a maximum value of about 2.5 at 10 K and then decreases to about 2 for temperatures slightly above 20 K. These 20 K values are essentially in agreement with the value of 2 normally adopted for interstellar dust [1]. The values of $\beta(T)$ determined for amorphous $MgO \cdot 2SiO_2$ display only a weak temperature dependence and the small value of 1.2 is in accord with values recently found for circumstellar particles, for example Refs. [12, 34] and references therein).

In summary these far infrared measurements show: (1) that the low temperature mass opacity coefficient of small amorphous $2MgO \cdot SiO_2$ and $MgO \cdot 2SiO_2$ grains are many times larger than the values previously used for interstellar grain material while that of $MgO \cdot SiO_2$ is found to be comparable; (2) that all of these silicate grains studied possess the characteristic temperature dependent signature associated with two level systems in bulk glass; and (3) that a smaller but nonzero two level temperature dependence signature is also observed for crystalline particles. The large magnitude of the observed low temperature absorption coefficient may be a consequence of non-stochiometry within the grain while the source of the temperature

dependence is resonant absorption by the glassy two level systems. More systematic studies including size dependent measurements will be required to determine if this effect is associated with the grain surfaces.

These laboratory measurements yield surprisingly large values for the mm-wave absorption coefficients of small particles similar to interstellar grains and suggest that the bulk absorptivity of interstellar dust at these long wavelengths will not be well known without such studies. Furthermore, it will be useful to understand the physics of the two level absorption process to gain confidence in the wide applicability of these results.

D. Extinction limits for a grain of arbitrary size and shape

The ubiquitous nature of the scattering and absorption of electromagnetic radiation by small particles has attracted scientific interest since the time of Tyndall and Lord Rayleigh. Whether one is examining aerosols in the atmosphere or starlight transmitted through interstellar dust, the extinction properties of the intervening particles need to be understood. By extinction one means absorption plus scattering since the extinction cross-section of a particle, in general, involves a subtle mix of scattering and absorption. Although coal smoke is black in the visible and water droplets are transparent, there are other frequency regions where the absorptive properties of these two different media are reversed, i.e., the coal smoke is transparent and the water is opaque. While the spectral properties of the ingredients in the particle are clearly important, its size and shape also play a key role. Absorption is the dominant factor in the extinction of a small particle and the spectral properties of such extinction are well understood. With increasing particle size compared to the wave length of the radiation, scattering becomes more significant and eventually dominates. The complexity of the scattering problem becomes apparent when one recognizes that the extinction cross section of a large opaque particle is equal to *twice* its geometrical cross section. The extra contribution comes about because of scattering at the particle edge. Given that a small particle may display spectral features in its extinction cross section characteristic of the bulk material while a large particle of the same material may only show a frequency independent extinction cross section over the same spectral region, it is intriguing that recently two general properties of the extinction spectrum have been found which characterize the electromagnetic properties of the particle *independent* of its scattering contribution.

A basic concept of response theory is that the particle cannot emit before the electromagnetic wave has arrived. This result and the general property that the extinction cross section is related to the scattering amplitude function in the forward direction (optical theorem) provide the building blocks with which one can demonstrate that the extinction cross section at some frequency is proportional to the plasma frequency squared contributed at that frequency. The plasma frequency is a particular combination of fundamental elements involved in the electromagnetic response, i.e., the number density, charge and mass of the charges involved. When all such frequency contributions are summed then the total strength, or plasma frequency squared, associated with the electromagnetic response of this medium is obtained[35, 36]. Since this sum is equal to the area under the extinction cross section spectrum, this "strength sum rule" which is independent of scattering and hence independent of the particle shape is particularly easy to visualize. The "dc polarizability sum rule"[37, 38] for the particle provides another constraint on the particle response since the extinction cross section divided by the frequency squared is

10

proportional to the static polarizability of the particle contributed at that frequency. Finally the ratio of these two sum rules produces a size-independent characteristic squared frequency of the extinction cross-section spectrum. All three of these results characterize and constrain the observable properties of the extinction spectrum.

To illustrate the properties of these sum rules for different size particles, the extinction cross section of spheres of single crystal silicon have been explored by computational methods since the complex refractive index of bulk silicon has been measured between 3.7 meV and 2 KeV[39]. The results for the volume normalized extinction cross section (Ext.) versus frequency are plotted in Fig. 5 for spheres with two very different diameters: 0.01 µm and 2.0 µm. Absorption is the dominant factor in the extinction cross section for the 0.01 µm diameter silicon sphere, and the corresponding extinction spectrum displays a resonance structure similar to the bulk material: a peak associated with interband transitions and L and K edges. Scattering becomes more important with increasing size, however, and it finally dominates for the 2.0 µm diameter sphere. Inspection of this extinction spectrum in Fig. 5 shows that it is nearly frequency independent over much of the interval (the L and K edges are now barely visible) with a value close to twice its geometrical cross section as expected for this limit. Although Fig. 5 demonstrates that the spectra produced by small and large spheres have little in common, according to the sum[40] rule the area under each of these curves is the same since the same material is involved.
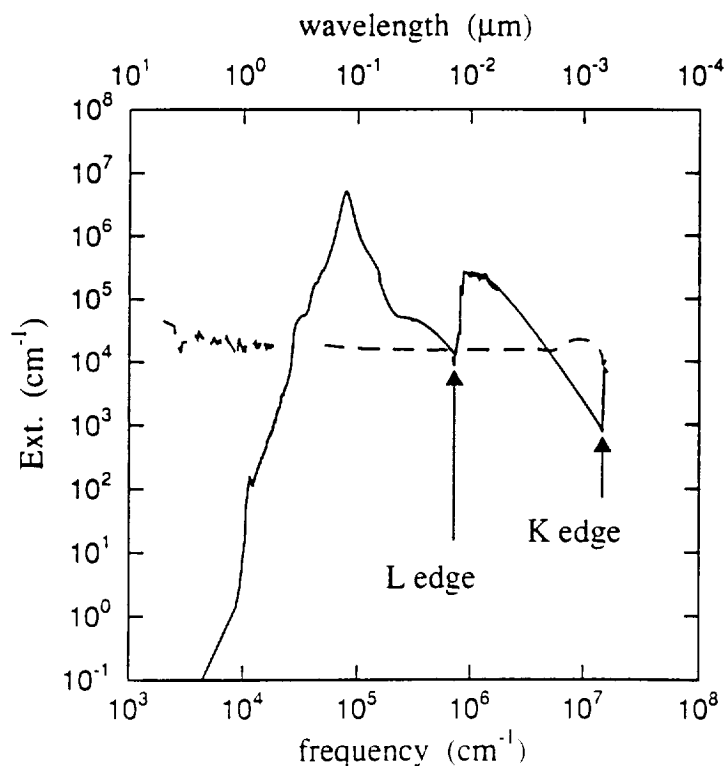

Figure 5. Volume normalized extinction cross section of single crystal silicon spheres vs frequency. The solid curve is for 0.01 µm diameter and the dashed curve is for 2.0 µm diameter.

Figure 6 shows the volume normalized frequency dependent extinction cross-section (Ext.) divided by the square of the frequency for the two sized particles. Again the two kinds of extinction spectra for small and large particles look dramatically different because they are produced by different mechanisms yet the area under each of these curves is again the same. When the area found in Fig. 5 is divided by the area found in Fig. 6 a third general property of the particle appears. It can be shown that this ratio depends only on the shape of the particle and the dc dielectric constant of the bulk medium from which the particle is made and not on the particle size.

Since the bulk dielectric constant of Si has not been measured above the K edge, the extinction spectrum of silicon spheres cannot be calculated above this value. The available data still provides a great deal of insight into the scattering problem. The procedure is to define effective sum rule values for Figs. 5 and 6 as a function of the upper limit of integration so that the ratio of the two gives a characteristic second moment frequency of the particle, $< \omega^2 >_{ext}$. If the complete frequency range is covered then this characteristic squared frequency is independent of particle size but if the frequency interval is finite the particle size enters. This difference between the two results is demonstrated in Fig. 7. Inspection of the results for the 0.01 µm diameter particle shows that with increasing frequency the characteristic squared frequency reaches a
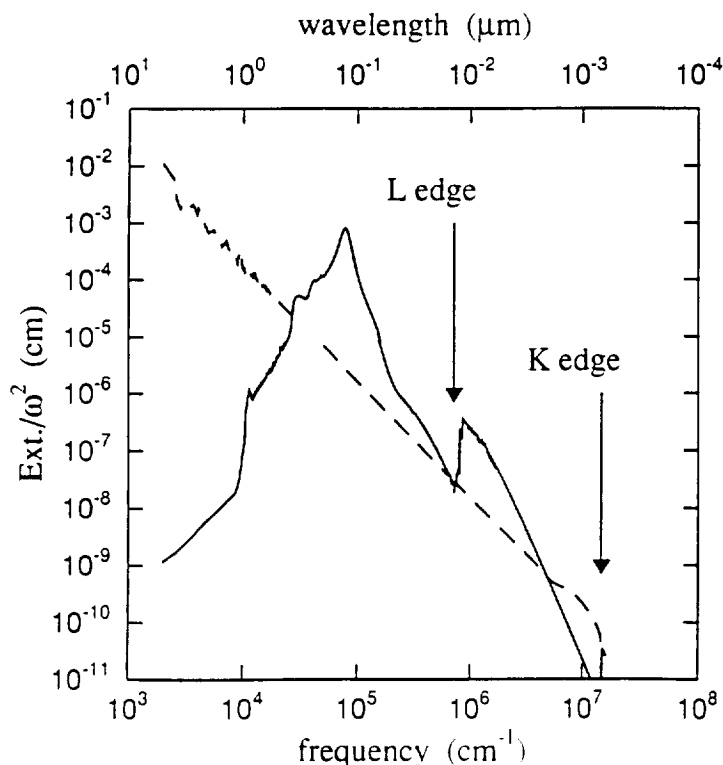

Figure 6. Volume normalized extinction cross section divided by frequency squared for single crystal silicon spheres vs frequency. The solid curve is for 0.01 µm diameter and the dashed curve is for 2.0 µm diameter.

12

plateau after the absorption band of bonding electrons is passed. It remains at this plateau value until the L-edge excitation threshold is reached whereupon the characteristic particle squared frequency increases again. It reaches another plateau after the absorption band of L electrons is passed and essentially remains at this value until the K-edge is reached. The contributions from the different electrons are well separated in frequency. For example, the L electrons produce no contribution to the absorption at frequencies below the L-edge, but do contribute to the real part of bulk dielectric function at lower frequencies. Since it is the real part of the dielectric function which enters in the scattering process, extinction curves for larger particles mix contributions from all electrons through scattering. Although the curve associated with the larger particle displays no spectral information about the bulk dielectric function, it is clear that this curve would reach the same value as for the small particle if the integration could be extended to a frequency above the K-edge. A similar analysis hold for nonspherical particles and particles embedded in an index matching medium[40].

This illustration with silicon particles of different sizes shows that although the extinction spectra of a small and a large particle made from the same bulk material are completely different, the two extinction sum rule values are conserved quantities independent of particle size. The strength sum rule is not only independent of particle size but also of particle shape while the dc sum rule is connected to the static polarizability, and hence to its shape.
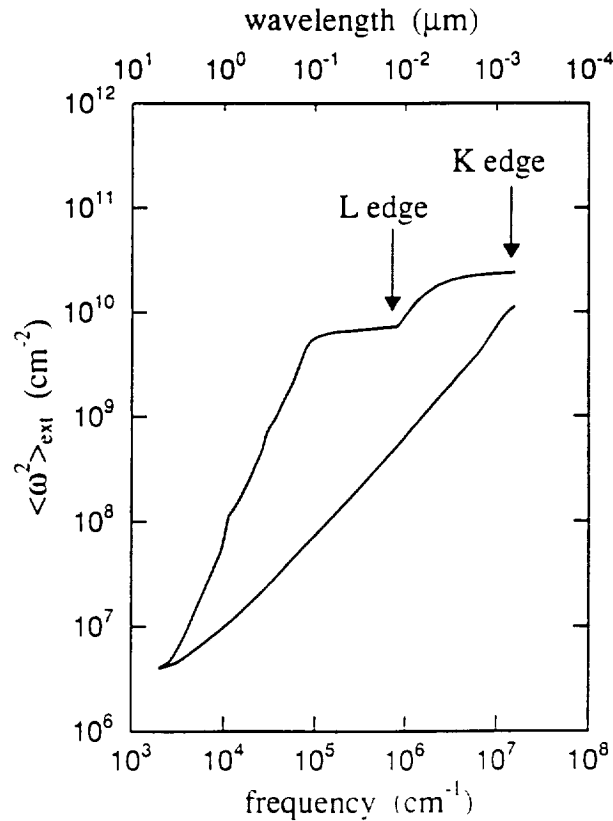

Figure 7. The characteristic second moment frequency of the particle.. $< \omega^2 >_{ext}$ vs frequency. The particle diameters are 0.01 μm and 2.0 μm for the two curves, top to bottom.

E. Publications resulting from the NASA award (1994-1997)

"Reassessment of millimeter-wave absorption coefficients in silicate grains," N. I. Agladze, A. J. Sievers, S. Jones, and S. V. W. Beckwith, Nature **372**, 243 (1994).

"Extinction Sum Rule and Optical Moment for an Ellipsoidal Particle of Arbitrary Size," A. J. Sievers, Optics Communication **109**, 71 (1994).

"Optical Moments and the Art of Dispersion Hardening," A. J. Sievers, T. W. Noh and J. B. Page, Physica A **207**, 46 (1994).

"Ultrafast Relaxation of the Fundamental Vibration of SH- in Potassium Halides," C.E. Mungan, U. Happek, J.T. McWhirter, and A.J. Sievers, J. of Luminescence **58**, 33 (1994).

"Frequency and Temperature Dependence of the Vibrational Relaxation of the SH Stretch Mode in Vitreous As_2S_3," U. Happek, J.R. Engholm and A. J. Sievers, Chem. Phys. Lett. **221**, 279 (1994).

"Characterization of the Optical Properties of Complex Systems," A. J. Sievers, J. of Solar Energy Materials and Solar Cells **32**, 451 (1994).

"Far-Infrared Properties of C_{60} and C_{70} Compacts," S. A. FitzGerald and A. J. Sievers, J. Chem. Phys. **101**, 7283 (1994).

"Infrared spectroscopy of the stretching modes of SeH⁻ and TeH⁻ in KCl and KBr: Cross sections, lifetimes and anharmonicities," C. E. Mungan, U. Happek, A. J. Sievers and T. Z. Hossain, J. Phys. Chem. Solids **56**, 735 (1995).

"Far IR Physics and the Processing of Optical Composites," A. J. Sievers, Proceedings of the International Conference on Millimeter and Submillimeter Waves and Applications, SPIE **2250**, 44 (1994).

"Far Infrared Absorption in Crystalline and Amorphous Forsterite Powders," N.I. Agladze, et al." Bull. Amer. Phys. Soc. **39**, 479 (1994).

"Two-level Systems and Excited-State Transitions in Fluorite Mixed Crystals and Silica Glass," S. A. FitzGerald, J. A. Campbell, and A. J. Sievers, Phys. Rev. Letters **73**, 3105 (1994).

"Two-level systems in glasses, mixed crystals and celestial solids," A. J. Sievers, S. A. FitzGerald, N. I. Agladze, J. A. Campbell, and S. V. W. Beckwith, 19th International Conference on Infrared and Millimeter Waves, K. Sakai and T. Yoneyama, eds., (Japan Society of Applied Physics, No. AP 941228, 1994), p. 275.

"Relaxation and IR Spectroscopic Properties of the CN- Stretching Mode in Silver Halides," C.E. Mungan, U. Happek, W. von der Osten, and A.J. Sievers, Rad. Effects Defects Solids **134**, 341 (1995).

"Mie Computational Test of the Extinction Cross-Section Sum Rules and Optical Moments for Large Dielectric Spheres and Shells," R. Lai and A. J. Sievers, Optics Communications **116**, 72 (1995).

"Observation of Site-Dependent Relaxation of the OH Vibrational Stretch Mode in Fused Silica, J.R. Engholm, U. Happek and A.J. Sievers, Chem. Phys. Letters **249**, 387 (1996).

"The Role of Network Topology on the Vibrational Relaxation of H2O Molecules in the Ge-As-Se Glass Series," B. Uebbing and A. J. Sievers, Phys. Rev. Lett. **76**, 932 (1996).

"Sum Rules and Optical Moments for a Course Scattering Medium," R. Lai and A. J. Sievers, Opt. Soc. of Am. A **13**, 1036 (1996).

"Laboratory Results on Millimeter-wave Absorption in Silicate Grain Materials at Cryogenic Temperatures," N. I. Agladze, A. J. Sievers, S. Jones, J. M. Burlitch, and S. V. W. Beckwith, Astrophysical Journal **462**, 1026-1040 (1996).

"Influence of the Glass Network on the Vibrational Energy Transfer from H_2O Impurities in the Ge-As-Se Glass Series," B. Uebbing and A. J. Sievers, J. NonCryst. Solids **202**, (1,2) (1996).

"MM-Wave Absorption by Two Level Systems in Mesoscopic Amorphous Grains," N. Agladze, A. J. Sievers, S. A. Jones and J. M. Burlitch, J. NonCryst. Solids **202**, (1,2) (1996).

"Persistent IR Spectral Hole Burning of the Vibrational Modes of H_2O in Chalcogenide Glasses," Gi. Schneider, B. Uebbing and A. J. Sievers, Mol. Cryst. Liq. Cryst. **291**, 235-240 (1996).

"The IR Vibrational Properties of Composite Solids and Particles: The Lyddane-Sachs-Teller Relation Revisited," A. J. Sievers, Spectroscopy and Dynamics of Collective Excitations in Solids, B. Di Bartolo, Ed., (Plenum Press, 1997).

14

F. References

1. B. T. Draine and H. M. Lee, "Optical properties of interstellar graphite and silicate grains", Ap. J. **421**, 89 (1984).
2. J. S. Mathis and G. Whiffen, "Composite interstellar grains", Ap. J. **341**, 808 (1989).
3. B. Draine, in *Proc. 22d ESLAB Symp. on Infrared Spectroscopy in Astronomy* B. H. Kaldeich, Ed. (ESA, Noordwiik, 1989) pp. 93.
4. D. C. B. Whittet, *Dust in the Galactic Environment*. R. J. Taylor and R. E. White, Eds., The Graduate Series in Astronomy (IOP Publishing, London, 1992).
5. J. S. Mathis, "Observations and theories of interstellar dust", Rep. Prog. Phys. **56**, 605 (1993).
6. B. T. Draine, "Dust in diffuse interstellar clouds", ASP Conference Series **58**, 227 (1994).
7. A. G. G. M. Tielens, D. H. Wooden, L. J. Allamandola, J. Bregman and F. C. Witteborn, "The infrared spectrum of the galactic center and the composition of interstellar dust", Ap. J **461**, 210 (1996).
8. J. P. Emerson, in *Formation and Evolution of Low Mass Stars* A. K. Dupree and M. T. V. T. Lago, Eds. (Kluwer Academic Publishers, Boston, 1988) pp. 21.
9. J. B. Pollack, D. Hollenbach, S. V. W. Beckwith, D. P. Simonelli, T. Rousch and W. Fong, "Composition and radiative properties of grains in molecular clouds and accretion disks", Ap. J. **421**, 615 (1994).
10. A. G. G. M. Tielens and L. J. Allamandola, in *Interstellar Processes* D. J. Hollenbach and H. A. Thronson, Eds. (D. Reidel Pub. Co., 1987) pp. 397.
11. S. V. W. Beckwith, A. I. Sargent and A. I. Chini, "A survey of circumstellar disks around young stellar objects", Astron. J. **99**, 924 (1990).
12. S. V. W. Beckwith and A. I. Sargent, "Particle emissivity in circumstellar disks", Ap. J. **381**, 250 (1991).
13. F. C. Adams, J. P. Emerson and G. A. Fuller, "Submillimeter photometry and disk masses of T Tauri disk systems", Ap. J. **357**, 606 (1990).
14. P. André, T. Montmerle, E. D. Feigelson and H. Steppe, "Cold dust around young stellar objects inn the rho Ophiuchi cloud core", Astro. & Astroph. **240**, 321 (1990).
15. E. L. Wright, J. C. Mather, C. L. Bennet, E. S. Cheng and e. al., "Preliminary spectral observations of the galaxy with a 7 degree beam by the cosmic background explorer", Ap. J. **381**, 200 (1991).
16. M. Rowin-Robinson, "On the nature of interstellar grains and the interpretation of the IRAS background radiation", M.N.R.A.S. **219**, 737 (1986).
17. R. H. Hildebrand, "The determination of cloud masses and dust characteristics from submillimeter thermal emission", Q.J.R.A.S. **24**, 267 (1983).
18. E. Bussoletti and L. Colangeli, "Cosmic Dust: from Space to laboratory", Riv. del Nuovo Cim. **13**. 1 (1990).
19. C. Jäger, H. Mutschke, B. Begemann, J. Dorschner and T. Henning, "Steps toward interstellar silicate minerology I. Laboratory results of a silicate glass of mean cosmic composition", Aston. Astro. **292**, 641 (1994).
20. J. M. Burlitch, M. L. Beeman, B. Riley and D. K. Kohlstedt, "Low temperature synthesis of olivine and forsterite facilitated by hydrogen peroxide", Chem. Mater. **3**, 692 (1991).
21. D. G. Park, J. C. Duchamp, T. M. Ducan and J. M. Burlitch, "Preparation of Fosterite by Pyrolysis of a Xerogel: The effect of water", Chem. Mater. **6**, 1990 (1994).
22. S. A. FitzGerald and A. J. Sievers, "Comment on 'Lattice Phonon Modes in Solid C60 Studied by Far-Infrared Spectroscopy'", Phys. Rev. Lett. **70**, 3175 (1993).
23. N. I. Agladze, A. J. Sievers, S. A. Jones, J. M. Birlitch and S. V. W. Beckwith, "Laboratory results on millimeter-wave absorption in silicate grain materials at cryogenic temperatures", Ap. J. **462**. 1026 (1996).
24. W. A. Phillips, "Two-level States in glasses", Rep. Prog. Phys. **50**, 1657 (1987).

25. K. K. Mon, Y. C. Chabal and A. J. Sievers, "Temperature dependence of the far-infrared absorption spectrum in amorphous dielectrics", Phys. Rev. Letters **35**, 1352 (1975).

26. S. A. FitzGerald, J. A. Campbell and A. J. Sievers, "Two-level systems and excited state transitions in fluorite mixed crystals and silica glass", Phys. Rev. Lett. **73**, 3105 (1994).

27. U. Strom and P. C. Taylor, "Temperature and frequency dependences of the far-infrared and microwave optical absorption in amorphous materials", Phys. Rev. B **16**, 5512 (1977).

28. M. A. Bösch, "Anomalous absorption in amorphous solids at low temperatures", Phys. Rev. Lett. **40**, 879 (1978).

29. P. W. Anderson, B. I. Halperin and C. M. Varma, "Anomalous low temperature thermal properties of glasses", Phil. Mag. **25**, 1 (1972).

30. M. von Schickfus, S. Hunklinger and I. Piché, "Anomalous dielectric dispersion in glasses at low temperatures", Phys. Rev. Lett. **35**, 876 (1975).

31. J. Fricke, in *Aerogels* J. Fricke, Ed.§Eds. (Springer-Verlag, Berlin, 1986), vol. 6, pp. 2.

32. J. Seki and T. Yamamoto, "Amorphous interstellar grains: Wavelength dependence of far-infrared emission efficiency", Astro. and Space Sci. **72**, 79 (1980).

33. E. Schlömann, "Dielectric losses in ionic crystals with disordered charge distributions", Phys. Rev. **135**, A413 (1964).

34. V. Manning and J. P. Emerson, "Dust in discs around T Tauri stars: grain growth?", M.N.R.A.S. **267**, 361 (1994).

35. A. J. Sievers, "Extinction Sum Rule and Optical Moment for an Ellipsoidal Particle of Arbitrary Size", Optics Commun. **109**, 71 (1994).

36. R. Lai and A. J. Sievers, "Mie computational test of the extinction cross-section sum rule and optical moments for large dielectric spheres and shells", Opt. Commun. **116**, 72 (1995).

37. E. M. Purcell, "On the absorption and emission of light by interstellar grains", Ap. J. **158**, 433 (1969).

38. C. F. Bohren and D. R. Huffman, *Absorption and Scattering of Light by Small Particles*. (John Wiley & Sons, New York, 1983).

39. D. F. Edwards, in *Handbook of Optical Constants of solids* E. D. Palik, Ed.§Eds. (Academic Press, New York, 1985) pp. 554.

40. R. Lai and A. J. Sievers, "Sum rules and optical moments for a coarse scattering medium", J. Opt. Soc. Am. A **13**, (1996).